



## Petrology of the Baszkówka L5 chondrite: A record of surface-forming processes on the parent body

Tadeusz Andrzej PRZYLIBSKI,<sup>1\*</sup> Andrzej Sylwester PILSKI<sup>2</sup>  
Paweł Przemysław ZAGOŹDŹON,<sup>3</sup> and Ryszard KRYZA<sup>4</sup>

<sup>1</sup>Wrocław University of Technology, Department of Mining, Division of Geology and Mineral Waters,  
Wybrzeże S. Wyspiańskiego 27, 50–370 Wrocław, Poland

<sup>2</sup>Nicholaus Copernicus Museum in Frombork, ul. Katedralna 8, 14–530 Frombork, Poland

<sup>3</sup>Wrocław University of Technology, Department of Mining, Division of Applied Geology, Dewatering and Ecology,  
Wybrzeże S. Wyspiańskiego 27, 50–370 Wrocław, Poland

<sup>4</sup>Wrocław University, Institute of Geological Sciences, Department of Mineralogy & Petrology  
ul. Cybulskiego 30, 50–205 Wrocław, Poland

\*Corresponding author. E-mail: [tadziop@chaos.ig.pwr.wroc.pl](mailto:tadziop@chaos.ig.pwr.wroc.pl)

(Received 9 July 2001; revision accepted 16 May 2003)

---

**Abstract**—We review the petrology of Baszkówka, present new microprobe data on mineral constituents, and propose a model for surface properties of the parent body consistent with these data.

The low shock index and high porosity of the Baszkówka L5 chondrite mean that considerable primary textural and petrographic detail is preserved, allowing insight into the structure and evolution of the parent body. This meteorite formed in a sedimentary environment resembling that in which pyroclastic rocks are deposited. The origin of the component chondrules, achondritic fragments (mostly olivine and pyroxene aggregates), chondritic-achondritic aggregates, and compound chondrules can be explained by invoking collision of 2 melted or partially melted planetesimals, each covered with a thin crust. This could have happened at an early stage in the evolution of the solar system, between 1 and 2 Myr after its origin. The collision resulted in the formation of a cloud containing products of earlier magmatic crystallization (chondrite and achondrite fragments) from which new chondrules were created. Particle collision in this cloud produced fragmented chondrules, chondritic-achondritic aggregates, and compound chondrules. Within this low-density medium, these particles were accreted on the surface of the larger of the planetesimals involved in the collision. The density of the medium was low enough to prevent grain-size sorting of the components but high enough to prevent the total loss of heat and to enable the welding of fragments on the surface of the body. The rock material was homogenized within the cloud and, in particular, within the zone close to the planetesimal surface. The hot material settled on the surface and became welded as molten or plastic metal, and sulfide components cemented the grains together. The process resembled the formation of welded ignimbrites. Once these processes on the planetesimal surface were completed, no subsequent recrystallization occurred. The high porosity of the Baszkówka chondrite indicates that the meteorite comes from a near-surface part of the parent body. Deeper parts of the planetesimal would have been more massive because of compaction.

---

### INTRODUCTION

The Baszkówka meteorite fell in the small village of Baszkówka, some 25 km southwest of Warsaw (Poland), around 4 p.m. on August 25, 1994. The fall was observed by several witnesses, which aided its find and subsequent studies. The results of these studies have recently been published (Stepniewski et al. 1996, 1997, 1998; Wlotzka et al.

1997; Przylibski and Zagożdżon 1999; Dybczyński et al. 1999, 2001a, b; Siemiątkowski 2001; Pilski et al. 2001; Borucki and Stepniewski 2001; Wlotzka and Otto 2001).

The textural features of this chondrite, and particularly its high porosity, are rarely found in meteorites and, consequently, have attracted much interest. The low shock index (S1) and immediate find of the meteorite make Baszkówka a unique object to study chondrites and the origin

of their parent bodies. The petrology of this meteorite clearly reflects the processes and environment of the formation of the parent body.

### PETROLOGY OF THE BASZKÓWKA L5 CHONDRITE

#### Summary of Published Data

The petrology of the Baszkówka chondrite has been intensely studied (Wlotzka et al. 1997; Przylibski and Zagożdżon 1999; Siemiątkowski 2001; Piłski et al. 2001). The meteorite is formed of: a) irregularly distributed automorphic compounds—chondrules, olivine, and pyroxene and plagioclase crystals; b) hipautomorphic particles—fragments of chondrules and olivine crystals; c) xenomorphic grains of metal (kamacite and taenite), troilite, and chromite; and d) accessory mackinavite and subordinate matrix (Stępniewski et al. 1997; Siemiątkowski 2001). The chondrules are represented by several types, some of which have secondary rims of strongly diversified composition. The chondrules and their fragments form ~30 vol% (locally up to 50%) of the rock. The remaining part comprises individual crystals of olivine (and pyroxene and plagioclase—see

below) as well as metal, troilite, and minor matrix. A considerable part of the meteorite volume comprises pores which form up to 20 vol% (Siemiątkowski 2001).

The most characteristic features of Baszkówka are numerous irregular pores (Figs. 1 and 2). Their diameter (up to 5 mm) is often larger than that of the largest chondrules and of automorphic olivine and pyroxene crystals. In places, the pores are interconnected and they form aligned systems (Fig. 1a–1c). Their size strongly suggests that the meteorite has not been compacted since the time of the parent rock formation. The grain framework of the meteorite is compact, although, all the grains loosely fill the rock volume (Figs. 1a–1c, 2a, and 2c). Locally, automorphic olivine and pyroxene crystals grow into the pore spaces (Fig. 2d), which may suggest their late crystallization (from pore fluid?), though, some represent original matrix fragments (Przylibski and Zagożdżon 1999). Euhedral crystals in interstitial pores of Baszkówka were analyzed in detail by Wlotzka and Otto (2001). Borucki and Stępniewski described zoning on alloys and troilite grain surfaces in the pores of the Baszkówka meteorite that may reflect interreactions with pore fluid (Borucki and Stępniewski 2001). No evidence exists that compaction and subsequent diagenetic processes occurred (Przylibski and Zagożdżon 1999).

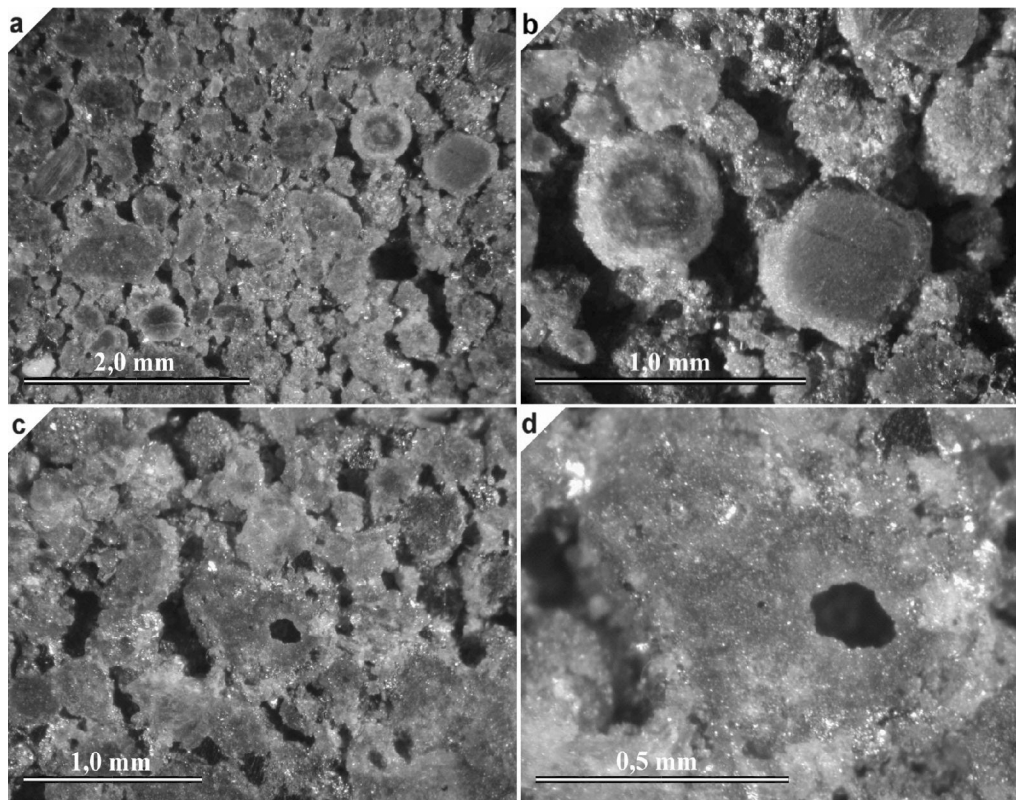


Fig. 1. Macroscopic views of the high porosity of the Baszkówka L5 chondrite: a) general view of the major components of the grain framework—chondrules accompanied by chondrule fragments and fine crystals of olivine, pyroxene, Fe-Ni alloys, and troilite, which form the highly porous fabric; b) close view of the chondrules and large pores between them; c) highly porous fabric that also contains an empty chondrule (in the center of the image); d) enlargement of the empty chondrule from the previous image.

The most abundant components of the framework are chondrules (Figs. 1a, 1b, 2b, 2c, 3a, 3c, and 4), chondrule fragments (Fig. 3b), and compound chondrules (Figs. 4c and 4d), which can be identified in their internal and external form. Small crystal aggregates, despite similarities to chondrule interiors, are not necessarily chondrule fragments. They may represent matrix where crystals and crystal aggregates have probably been produced by resublimation and which have never formed parts of chondrules. This theory is supported by the observations that crystals (Figs. 3c, 5c, and 5d) and crystalline aggregates of olivine and pyroxene are as large as the largest chondrules, and equigranular textures (Figs. 3d, 5a, and 5b) lack features typical of chondrules. Both of these compounds are also of low porosity in relation to the rest of the rock. Similar features are characteristic also of aggregates comprised of chondrules, chondrule fragments, and individual olivine and pyroxene crystals. Most likely, both of these aggregate types are equivalent to chondrules and to chondrule fragments in that they had been assembled before the meteorite was formed (Figs. 2c, 3d, 4a, 4b, and 4f). Larger xenomorphic grains of Fe-Ni alloys and troilite are also considered as components of the grain framework of the meteorite (Przylibski and Zagożdżon 1999).

The chondrules must have fragmented before the formation of the meteorite, as no matching fragments of chondrules have been found. This inference is supported by

the presence of accretionary rims not only on their original spherical surfaces, but also on broken surfaces. Accretionary rims are relatively thin along the broken surfaces, suggesting a relatively short time between the collision that fragmented the chondrules and the formation of the new rock. Collision can also be inferred from the observed textural interrelationships between chondrules and relatively large hipautomorphic olivine crystals (Fig. 4a), fine-crystalline olivine aggregates (Figs. 5a and 5b), or Fe-Ni alloy grains (Figs. 4b and 4f) and compound chondrules (Figs. 4c and 4d). All these processes took place before the formation of the parent body (Przylibski and Zagożdżon 1999).

The matrix is composed of small chondrule fragments, small grains of Fe-Ni alloy and troilite, and individual small auto- and hipautomorphic crystals of olivine (Fig. 4). Its volume is subordinate to the dominant grain framework and to the pore space (Przylibski and Zagożdżon 1999). The parent rock of the chondrite contains practically no cement, but Fe-Ni alloys and troilite may have a significant bonding effect. However, most bonding took place at grain boundaries (mainly between chondrules and their fragments) where limited recrystallization may have occurred. This represents a form of regeneration cement, and joining the grains of the framework can be seen as “welding” of hot and partly plastic (Fe-Ni alloys and troilite) components (Przylibski and Zagożdżon 1999). The process may be similar to that of

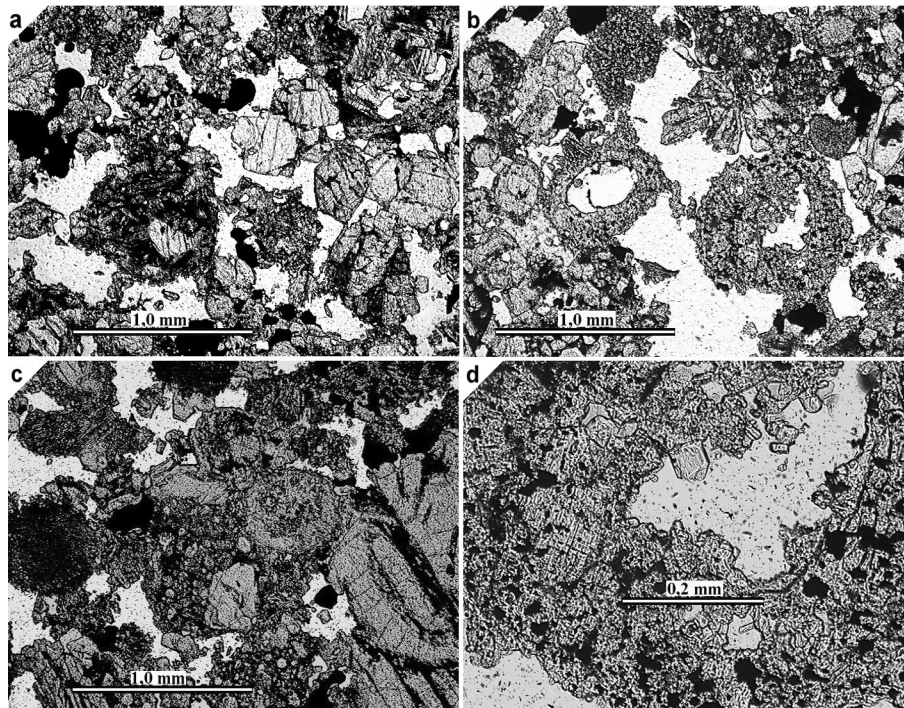


Fig. 2. The fabric of the Baszkówka L5 chondrite: a) pore spaces (bright) between loosely located components of the grain framework and matrix. Transmitted plane polarized light; b) interconnected pore system and “empty” chondrules. Small, undeformed olivine crystals grow into the pore spaces. Transmitted plane polarized light; c) loose grain framework and minor matrix. The fragment composed of chondrules and achondritic fragments in the center of the image must have formed before the Baszkówka parent body was created. Transmitted plane polarized light; d) small olivine crystals growing into the pore space. Transmitted plane polarized light.

terrestrial pyroclastic rocks, in which the pyroclastic grains may be welded after deposition.

The parent rock of the Baszkówka chondrite may be compared petrologically to a polymictic sandstone with a compact grain framework and a minor amount of matrix and cement. Both the framework and matrix are composed of allogenic grains. The rock is medium- to coarse-grained and locally resembles a conglomeratic sandstone with a poorly sorted framework. The texture is syngenetic, random, and porous. The rock has been labeled a chondritic sandstone (Przylibski and Zagożdżon 1999), although, “chondrule sandstone” may be a more adequate name, if classified as a sedimentary rock.

### New Electron Microprobe Work: Scope and Techniques

The mineralogy and mineral chemistry of the Baszkówka L5 chondrite have been extensively studied, and the results have been published elsewhere (see references above). Our electron microprobe work focused on the possible variation in mineral and chemical composition of mineral grains exposed on pore surfaces compared to those enclosed within chondrules and within the massive matrix. Such observations may illuminate the physical and chemical conditions of the meteorite formation processes.

The electron microprobe work was performed using the Cambridge M9 Microscan at the Department of Mineralogy and Petrology, Institute of Geological Sciences at Wrocław University. The measurements were obtained from one polished slide,  $\sim 2 \times 2$  cm in size, and they included: BSE and EDS X-ray element distribution images, and quantitative analyses made by 2 WDS spectrometers calibrated with natural and synthetic standards. Iron was calibrated separately for various phases: on garnet for silicate analyses, on troilite for sulfides, and on Fe metal for kamacite and taenite. The analytical conditions were: accelerating voltage 15 kV, beam current 50 nA, counting time 15 sec, focused beam (1–2 microns) and ZAF correction.

### Summary of New Results

Representative new microprobe analyses (selected from a set of  $\sim 50$  analytical points) are given in Table 1. The new results can be summarized as follows:

- Olivine is the most abundant component of the chondrite. It displays a “spongy” texture intensely intergrown with a “network” of plagioclase which comprises up to 30–40 vol% of the intergrowths. On the pore surfaces, mineral grain boundaries are highly irregular resembling “cauliflower textures.” The central parts of some olivine

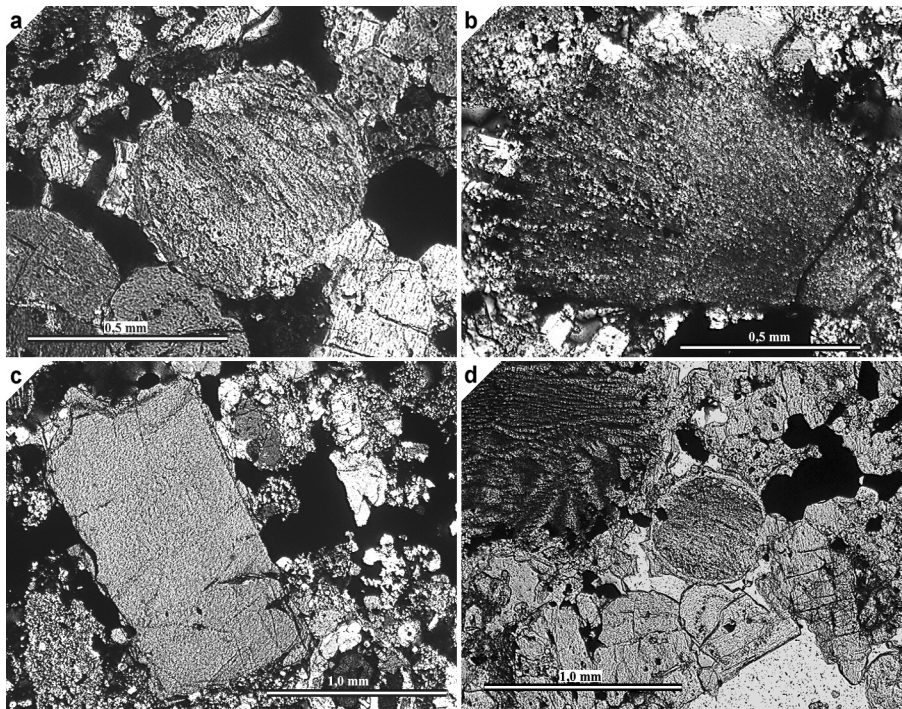


Fig. 3. The components of the grain framework of the Baszkówka chondrite: a) polyspherulitic chondrule with an accretionary rim. Transmitted light, crossed polars; b) broken monospherulitic chondrule. Transmitted light, crossed polars; c) large olivine crystal. Transmitted light, crossed polars; d) polyspherulitic chondrule with accretionary rim (in the center of the photo) and olivine crystalline aggregate (below the center). Transmitted plane polarized light.

Table 1. Chemical composition (wt%) of minerals of the Baszkówka L5 chondrite. The final chemical composition of silicates (olivine, pyroxene, plagioclase) is expressed in mol% of: Fo, Fa, and Te (olivine); Fs, Wo, and En (pyroxene); Ab, Or, and An (plagioclase).

| Olivine                        |        |        |        |       |        |        |                                |        |        |        |        |        |        |
|--------------------------------|--------|--------|--------|-------|--------|--------|--------------------------------|--------|--------|--------|--------|--------|--------|
| Analysis                       | WOD    | WOA    | WOF    | WOG   | WOJ    | WOK    | WON                            | WOP    | WOQ    | WOU    | WOV    | WOW    | Mean   |
| Core/rim                       | r      | c      | c      | r     | r      | c      | r                              | c      | c      | c      | r      |        |        |
| SiO <sub>2</sub>               | 39.04  | 39.24  | 39.81  | 39.28 | 39.74  | 39.51  | 39.67                          | 39.10  | 39.47  | 39.59  | 39.62  | 39.48  | 39.46  |
| TiO <sub>2</sub>               | 0.00   | 0.02   | 0.00   | 0.00  | 0.00   | 0.00   | 0.00                           | 0.00   | 0.00   | 0.00   | 0.00   | 0.00   | 0.00   |
| Al <sub>2</sub> O <sub>3</sub> | 0.16   | 0.16   | 0.05   | 0.18  | 0.07   | 0.25   | 0.14                           | 0.23   | 0.07   | 0.05   | 0.09   | 0.11   | 0.13   |
| Cr <sub>2</sub> O <sub>3</sub> | 0.00   | 0.00   | 0.00   | 0.00  | 0.00   | 0.00   | 0.00                           | 0.00   | 0.00   | 0.00   | 0.00   | 0.00   | 0.00   |
| FeO                            | 22.79  | 22.42  | 23.79  | 23.00 | 23.26  | 23.55  | 23.79                          | 22.50  | 23.51  | 23.13  | 23.00  | 23.10  | 23.15  |
| MnO                            | 0.44   | 0.56   | 0.52   | 0.55  | 0.58   | 0.55   | 0.48                           | 0.53   | 0.56   | 0.48   | 0.55   | 0.58   | 0.53   |
| NiO                            | 0.01   | 0.07   | 0.01   | 0.00  | 0.01   | 0.00   | 0.06                           | 0.00   | 0.00   | 0.01   | 0.01   | 0.01   | 0.02   |
| MgO                            | 36.43  | 37.50  | 37.65  | 36.81 | 37.52  | 36.80  | 35.99                          | 37.30  | 36.35  | 37.33  | 37.60  | 37.01  | 37.02  |
| CaO                            | 0.00   | 0.00   | 0.01   | 0.04  | 0.00   | 0.01   | 0.01                           | 0.01   | 0.03   | 0.00   | 0.00   | 0.01   | 0.01   |
| Na <sub>2</sub> O              | 0.15   | 0.23   | 0.02   | 0.00  | 0.00   | 0.00   | 0.07                           | 0.07   | 0.10   | 0.20   | 0.05   | 0.00   | 0.07   |
| Total                          | 99.02  | 100.20 | 101.86 | 99.86 | 101.18 | 100.67 | 100.21                         | 99.74  | 100.09 | 100.79 | 100.92 | 100.30 | 100.40 |
| Si <sup>+4</sup>               | 1.026  | 1.018  | 1.019  | 1.024 | 1.022  | 1.023  | 1.033                          | 1.019  | 1.028  | 1.023  | 1.021  | 1.024  | 1.023  |
| Ti <sup>+4</sup>               | 0.000  | 0.000  | 0.000  | 0.000 | 0.000  | 0.000  | 0.000                          | 0.000  | 0.000  | 0.000  | 0.000  | 0.000  | 0.000  |
| Al <sup>+3</sup>               | 0.005  | 0.005  | 0.002  | 0.006 | 0.002  | 0.008  | 0.004                          | 0.007  | 0.002  | 0.002  | 0.003  | 0.003  | 0.004  |
| Cr <sup>+3</sup>               | 0.000  | 0.000  | 0.000  | 0.000 | 0.000  | 0.000  | 0.000                          | 0.000  | 0.000  | 0.000  | 0.000  | 0.000  | 0.000  |
| Fe <sup>+2</sup>               | 0.501  | 0.486  | 0.509  | 0.501 | 0.500  | 0.510  | 0.518                          | 0.490  | 0.512  | 0.500  | 0.496  | 0.501  | 0.502  |
| Mn <sup>+2</sup>               | 0.010  | 0.012  | 0.011  | 0.012 | 0.013  | 0.012  | 0.011                          | 0.012  | 0.012  | 0.011  | 0.012  | 0.013  | 0.012  |
| Ni <sup>+2</sup>               | 0.000  | 0.001  | 0.000  | 0.000 | 0.000  | 0.000  | 0.001                          | 0.000  | 0.000  | 0.000  | 0.000  | 0.000  | 0.000  |
| Mg <sup>+2</sup>               | 1.427  | 1.450  | 1.437  | 1.430 | 1.439  | 1.420  | 1.397                          | 1.448  | 1.412  | 1.437  | 1.445  | 1.432  | 1.431  |
| Ca <sup>+2</sup>               | 0.000  | 0.000  | 0.000  | 0.001 | 0.000  | 0.000  | 0.000                          | 0.000  | 0.001  | 0.000  | 0.000  | 0.000  | 0.000  |
| Na <sup>+</sup>                | 0.008  | 0.012  | 0.001  | 0.000 | 0.000  | 0.000  | 0.004                          | 0.004  | 0.005  | 0.010  | 0.002  | 0.000  | 0.004  |
| Total                          | 2.976  | 2.985  | 2.980  | 2.974 | 2.977  | 2.973  | 2.967                          | 2.980  | 2.973  | 2.982  | 2.979  | 2.974  | 2.977  |
| O-2                            | 4.000  | 4.000  | 4.000  | 4.000 | 4.000  | 4.000  | 4.000                          | 4.000  | 4.000  | 4.000  | 4.000  | 4.000  | 4.000  |
| X Mg                           | 0.74   | 0.75   | 0.74   | 0.74  | 0.74   | 0.74   | 0.73                           | 0.75   | 0.73   | 0.74   | 0.74   | 0.74   | 0.74   |
| Fo                             | 73.65  | 74.41  | 73.40  | 73.58 | 73.72  | 73.13  | 72.55                          | 74.27  | 72.91  | 73.81  | 73.99  | 73.58  | 73.58  |
| Fa                             | 25.85  | 24.96  | 26.02  | 25.79 | 25.64  | 26.25  | 26.90                          | 25.13  | 26.45  | 25.65  | 25.39  | 25.76  | 25.82  |
| Te                             | 0.51   | 0.63   | 0.58   | 0.62  | 0.65   | 0.62   | 0.55                           | 0.60   | 0.64   | 0.54   | 0.61   | 0.66   | 0.60   |
| Pyroxene                       |        |        |        |       |        |        | Plagioclase                    |        |        |        |        |        |        |
| Analysis                       | WOH    | WOO    | WOS    | WOT   | WOM    | Mean   | Analysis                       | WPD    | WPE    | WPF    | Mean   |        |        |
| Core/rim                       | c      | c      | c      | r     |        |        | Core/rim                       |        |        |        |        |        |        |
| SiO <sub>2</sub>               | 57.33  | 57.18  | 56.86  | 57.00 | 55.38  | 56.75  | SiO <sub>2</sub>               | 66.20  | 63.82  | 65.39  | 65.14  |        |        |
| Al <sub>2</sub> O <sub>3</sub> | 0.32   | 0.21   | 0.34   | 0.21  | 0.30   | 0.28   | Al <sub>2</sub> O <sub>3</sub> | 20.35  | 21.78  | 20.47  | 20.87  |        |        |
| FeO                            | 14.30  | 14.25  | 14.32  | 13.89 | 15.34  | 14.42  | FeO                            | 1.66   | 1.84   | 2.31   | 1.94   |        |        |
| MnO                            | 0.51   | 0.52   | 0.49   | 0.41  | 0.54   | 0.49   | MgO                            | 1.28   | 0.63   | 0.27   | 0.73   |        |        |
| NiO                            | 0.00   | 0.00   | 0.01   | 0.01  | 0.00   | 0.00   | MnO                            | 0.05   | 0.00   | 0.03   | 0.03   |        |        |
| MgO                            | 27.59  | 27.52  | 27.24  | 26.90 | 28.50  | 27.55  | CaO                            | 2.26   | 2.21   | 2.54   | 2.34   |        |        |
| CaO                            | 0.97   | 0.90   | 0.71   | 0.81  | 0.63   | 0.80   | Na <sub>2</sub> O              | 8.36   | 9.19   | 10.20  | 9.25   |        |        |
| Na <sub>2</sub> O              | 0.00   | 0.09   | 0.09   | 0.11  | 0.00   | 0.06   | K <sub>2</sub> O               | 1.07   | 0.98   | 0.67   | 0.91   |        |        |
| Total                          | 101.02 | 100.67 | 100.06 | 99.34 | 100.69 | 100.36 | Total                          | 101.23 | 100.45 | 101.88 | 101.19 |        |        |
| Si <sup>+4</sup>               | 2.026  | 2.028  | 2.029  | 2.043 | 1.981  | 2.021  | Si <sup>+4</sup>               | 2.895  | 2.828  | 2.869  | 2.864  |        |        |
| Al <sup>+3</sup>               | 0.013  | 0.009  | 0.014  | 0.009 | 0.013  | 0.012  | Al <sup>+3</sup>               | 1.049  | 1.138  | 1.058  | 1.082  |        |        |
| Fe <sup>+2</sup>               | 0.423  | 0.423  | 0.427  | 0.416 | 0.459  | 0.430  | Fe <sup>+2</sup>               | 0.061  | 0.068  | 0.085  | 0.071  |        |        |
| Mn <sup>+2</sup>               | 0.015  | 0.016  | 0.015  | 0.012 | 0.016  | 0.015  | Mg <sup>+2</sup>               | 0.083  | 0.042  | 0.018  | 0.048  |        |        |
| Ni <sup>+2</sup>               | 0.000  | 0.000  | 0.000  | 0.000 | 0.000  | 0.000  | Mn <sup>+2</sup>               | 0.002  | 0.000  | 0.001  | 0.001  |        |        |
| Mg <sup>+2</sup>               | 1.453  | 1.455  | 1.449  | 1.437 | 1.520  | 1.463  | Ca <sup>+2</sup>               | 0.106  | 0.105  | 0.119  | 0.110  |        |        |
| Ca <sup>+2</sup>               | 0.037  | 0.034  | 0.027  | 0.031 | 0.024  | 0.031  | Na <sup>+</sup>                | 0.709  | 0.790  | 0.868  | 0.789  |        |        |
| Na <sup>+</sup>                | 0.000  | 0.006  | 0.006  | 0.008 | 0.000  | 0.004  | K <sup>+</sup>                 | 0.060  | 0.055  | 0.037  | 0.051  |        |        |
| Total                          | 3.967  | 3.971  | 3.967  | 3.957 | 4.013  | 3.975  | Total                          | 4.965  | 5.026  | 5.055  | 5.015  |        |        |
| O-2                            | 6.000  | 6.000  | 6.000  | 6.000 | 6.000  | 6.000  | O-2                            | 8.000  | 8.000  | 8.000  | 8.000  |        |        |
| Fs                             | 22.09  | 22.11  | 22.45  | 22.09 | 22.91  | 22.33  | Ab                             | 81.06  | 83.12  | 84.69  | 82.96  |        |        |
| Wo                             | 1.92   | 1.79   | 1.43   | 1.65  | 1.21   | 1.60   | Or                             | 6.83   | 5.83   | 3.66   | 5.44   |        |        |
| En                             | 75.99  | 76.10  | 76.12  | 76.26 | 75.88  | 76.07  | An                             | 12.11  | 11.05  | 11.65  | 11.60  |        |        |

Table 1. Chemical composition (wt%) of minerals of the Baszkówka L5 chondrite. The final chemical composition of silicates (olivine, pyroxene, plagioclase) is expressed in mol% of: Fo, Fa, and Te (olivine); Fs, Wo, and En (pyroxene); Ab, Or, and An (plagioclase). *Continued.*

| Troilite         |       |        |       |        |       |       |        |        |        |       | Chromite                       |       |       |       |
|------------------|-------|--------|-------|--------|-------|-------|--------|--------|--------|-------|--------------------------------|-------|-------|-------|
| Analysis         | WTA   | WTB    | WTC   | WTD    | WTE   | WTF   | WTG    | WTH    | WTI    | Mean  | Analysis                       | WMM   | WMN   | Mean  |
| Core/rim         | c     | r      | c     | r      | r     | c     | c      | c      | r      |       | Core/rim                       |       |       |       |
| Si               | 0.45  | 0.03   | 0.04  | 0.03   | 0.06  | 0.08  | 0.02   | 0.02   | 0.04   | 0.09  | SiO <sub>2</sub>               | 0.26  | 0.16  | 0.21  |
| Ti               | 0.00  | 0.00   | 0.02  | 0.00   | 0.01  | 0.00  | 0.01   | 0.00   | 0.00   | 0.00  | TiO <sub>2</sub>               | 3.13  | 3.13  | 3.13  |
| Al               | 0.02  | 0.04   | 0.12  | 0.06   | 0.02  | 0.03  | 0.02   | 0.02   | 0.03   | 0.04  | Al <sub>2</sub> O <sub>3</sub> | 5.75  | 5.90  | 5.83  |
| Cr               | 0.01  | 0.00   | 0.01  | 0.00   | 0.00  | 0.01  | 0.01   | 0.01   | 0.00   | 0.01  | Cr <sub>2</sub> O <sub>3</sub> | 56.19 | 56.39 | 56.29 |
| Fe               | 63.69 | 64.61  | 63.71 | 64.57  | 63.75 | 63.59 | 64.56  | 64.69  | 64.68  | 64.21 | FeO                            | 30.73 | 30.67 | 30.70 |
| Mn               | 0.03  | 0.02   | 0.03  | 0.00   | 0.01  | 0.10  | 0.01   | 0.01   | 0.02   | 0.03  | MnO                            | 0.49  | 0.56  | 0.53  |
| Ni               | 0.04  | 0.00   | 0.00  | 0.01   | 0.00  | 0.51  | 0.00   | 0.00   | 0.00   | 0.06  | MgO                            | 2.63  | 2.49  | 2.56  |
| Mg               | 0.40  | 0.04   | 0.03  | 0.01   | 0.04  | 0.05  | 0.01   | 0.03   | 0.03   | 0.07  | Total                          | 99.18 | 99.30 | 99.24 |
| Ca               | 0.03  | 0.00   | 0.00  | 0.00   | 0.00  | 0.00  | 0.00   | 0.00   | 0.00   | 0.00  | Si <sup>+4</sup>               | 0.009 | 0.006 | 0.007 |
| Na               | 0.09  | 0.03   | 0.00  | 0.00   | 0.00  | 0.00  | 0.00   | 0.00   | 0.00   | 0.01  | Ti <sup>+4</sup>               | 0.084 | 0.084 | 0.084 |
| S                | 34.73 | 35.59  | 35.21 | 35.72  | 35.23 | 34.82 | 35.76  | 35.27  | 35.48  | 35.31 | Al <sup>+3</sup>               | 0.242 | 0.248 | 0.245 |
| Total            | 99.49 | 100.36 | 99.17 | 100.40 | 99.12 | 99.19 | 100.40 | 100.05 | 100.28 | 99.83 | Cr <sup>+3</sup>               | 1.586 | 1.590 | 1.588 |
| Si <sup>+4</sup> | 0.014 | 0.001  | 0.001 | 0.001  | 0.002 | 0.003 | 0.001  | 0.001  | 0.001  | 0.003 | Fe <sup>+2</sup>               | 0.917 | 0.915 | 0.916 |
| Ti <sup>+4</sup> | 0.000 | 0.000  | 0.000 | 0.000  | 0.000 | 0.000 | 0.000  | 0.000  | 0.000  | 0.000 | Mn <sup>+2</sup>               | 0.015 | 0.017 | 0.016 |
| Al <sup>+3</sup> | 0.001 | 0.001  | 0.004 | 0.002  | 0.001 | 0.001 | 0.001  | 0.001  | 0.001  | 0.001 | Mg <sup>+2</sup>               | 0.140 | 0.132 | 0.136 |
| Cr <sup>+3</sup> | 0.000 | 0.000  | 0.000 | 0.000  | 0.000 | 0.000 | 0.000  | 0.000  | 0.000  | 0.000 | Total                          | 2.993 | 2.991 | 2.992 |
| Fe <sup>+2</sup> | 1.008 | 1.018  | 1.015 | 1.017  | 1.017 | 1.016 | 1.017  | 1.024  | 1.021  | 1.017 | O-2                            | 4.000 | 4.000 | 4.000 |
| Mn <sup>+2</sup> | 0.000 | 0.000  | 0.000 | 0.000  | 0.000 | 0.002 | 0.000  | 0.000  | 0.000  | 0.000 |                                |       |       |       |
| Ni <sup>+2</sup> | 0.001 | 0.000  | 0.000 | 0.000  | 0.000 | 0.008 | 0.000  | 0.000  | 0.000  | 0.001 |                                |       |       |       |
| Mg <sup>+2</sup> | 0.015 | 0.001  | 0.001 | 0.000  | 0.001 | 0.002 | 0.000  | 0.001  | 0.001  | 0.003 |                                |       |       |       |
| Ca <sup>+2</sup> | 0.001 | 0.000  | 0.000 | 0.000  | 0.000 | 0.000 | 0.000  | 0.000  | 0.000  | 0.000 |                                |       |       |       |
| Na <sup>+</sup>  | 0.003 | 0.001  | 0.000 | 0.000  | 0.000 | 0.000 | 0.000  | 0.000  | 0.000  | 0.001 |                                |       |       |       |
| S-2              | 0.957 | 0.977  | 0.977 | 0.980  | 0.979 | 0.969 | 0.981  | 0.973  | 0.975  | 0.974 |                                |       |       |       |
| Total            | 2.000 | 2.000  | 2.000 | 2.000  | 2.000 | 2.000 | 2.000  | 2.000  | 2.000  | 2.000 |                                |       |       |       |
| Charge           | 0.196 | 0.095  | 0.098 | 0.085  | 0.090 | 0.130 | 0.078  | 0.110  | 0.102  | 0.109 |                                |       |       |       |

| Kamacite <sup>a</sup> |       |       |        |       |       |       |       | Taenite  |        |        |        |        |                   |
|-----------------------|-------|-------|--------|-------|-------|-------|-------|----------|--------|--------|--------|--------|-------------------|
| Analysis              | WMA   | WMB   | WMC    | WMD   | WME   | WMH   | Mean  | Analysis | WMK    | WMI    | WMJ    | WML    | Mean <sup>b</sup> |
| Core/rim              | r     | c     | r      | c     | r     |       |       | Core/rim | r      | c      | r      | c      |                   |
| Si                    | 0.06  | 0.03  | 0.03   | 0.06  | 0.05  | 0.06  | 0.05  | Si       | 0.08   | 0.04   | 0.04   | 0.05   | 0.04              |
| Ti                    | 0.00  | 0.00  | 0.00   | 0.01  | 0.00  | 0.00  | 0.00  | Ti       | 0.00   | 0.01   | 0.01   | 0.02   | 0.01              |
| Al                    | 0.10  | 0.05  | 0.05   | 0.10  | 0.07  | 0.10  | 0.08  | Al       | 0.05   | 0.07   | 0.11   | 0.08   | 0.09              |
| Cr                    | 0.00  | 0.00  | 0.00   | 0.00  | 0.00  | 0.00  | 0.00  | Cr       | 0.02   | 0.00   | 0.01   | 0.00   | 0.00              |
| Fe                    | 92.64 | 93.12 | 93.97  | 93.62 | 93.81 | 92.73 | 93.32 | Fe       | 86.61  | 75.25  | 75.07  | 76.35  | 75.56             |
| Mn                    | 0.00  | 0.02  | 0.01   | 0.00  | 0.02  | 0.01  | 0.01  | Mn       | 0.01   | 0.04   | 0.00   | 0.00   | 0.01              |
| Ni                    | 5.66  | 5.94  | 5.98   | 5.99  | 5.87  | 6.39  | 5.97  | Ni       | 13.58  | 25.82  | 25.69  | 24.58  | 25.36             |
| Mg                    | 0.03  | 0.03  | 0.03   | 0.06  | 0.01  | 0.04  | 0.03  | Mg       | 0.03   | 0.03   | 0.03   | 0.03   | 0.03              |
| Ca                    | 0.25  | 0.00  | 0.00   | 0.00  | 0.00  | 0.11  | 0.06  | Ca       | 0.00   | 0.00   | 0.00   | 0.00   | 0.00              |
| Na                    | 0.00  | 0.02  | 0.00   | 0.00  | 0.00  | 0.00  | 0.00  | Na       | 0.00   | 0.00   | 0.00   | 0.00   | 0.00              |
| S                     | 0.01  | 0.00  | 0.01   | 0.00  | 0.01  | 0.01  | 0.01  | S        | 0.02   | 0.01   | 0.01   | 0.01   | 0.01              |
| Total                 | 98.75 | 99.21 | 100.08 | 99.84 | 99.84 | 99.45 | 99.53 | Total    | 100.40 | 101.27 | 100.97 | 101.12 | 101.12            |

<sup>a</sup>Missed during electron microprobe examinations, Co concentrations in kamacite are between 1.07 and 1.66 wt% (Borucki and Stępniewski 2001).

<sup>b</sup>Mean of the analyses WMI, WMJ, and WML.

grains contain regular lamellar intergrowths of plagioclase 10–50 μm thick. In places, small crystals of olivine project into the pore space; they are euhedral to subhedral in shape, often with slightly rounded edges. The chemical composition of the olivine is fairly constant and independent of its textural location: Fo ~73, Fa ~26, and Te ~0.6 mol%. The main admixtures are Al<sub>2</sub>O<sub>3</sub>, CaO, and Na<sub>2</sub>O, all apparently more abundant in grains that are exposed at pore boundaries.

- Pyroxene has been found to be a common component associated with the olivine. It forms more massive, locally subhedral to euhedral crystals that are less

penetrated by plagioclase. The grain boundaries exposed on pore surfaces are similar to those of olivine, although, in the pyroxene, they tend to be more regular. The chemical composition of the pyroxene is also fairly constant: En ~76, Fs ~22, and Wo 1.2–1.9 mol%. Small pyroxene crystals on pore surfaces seem to contain slightly more Fe and less Ca compared with the average pyroxene composition.

- Plagioclase penetrating both the olivine and pyroxene and, less commonly, forming small and rather isometric grains, shows no significant chemical variation and contains: Ab 81–84, Or 4–7, and An 11–12 mol%. The

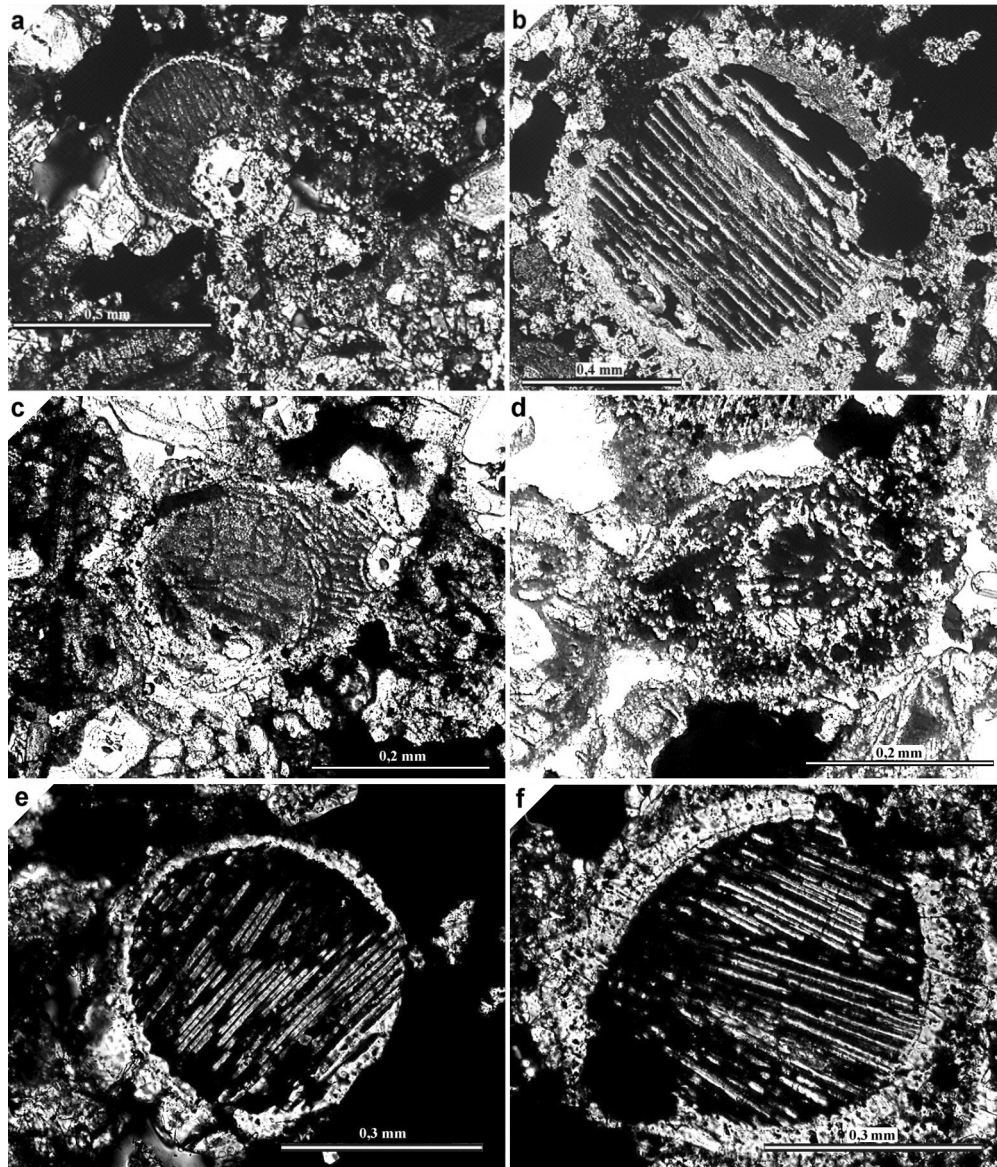


Fig. 4. Evidences of chondritic and achondritic pyroclasts' binding process and formation of the accretionary rims of chondrules before the process of accretion on the planetesimal surface: a) aggregate composed of a polyspherulitic chondrule with an impacted hipautomorphic olivine crystal. Transmitted light, crossed polars; b) barred chondrule with an accretionary rim which also covers a grain of Fe-Ni alloy impacted into the chondrule (probably due to collision postdating chondrule formation). Transmitted light, crossed polars; c) compound chondrule created as a result of the collision between 2 chondrules during their falling onto the planetesimal surface. Transmitted plane polarized light; d) compound chondrule—a smaller chondrule is incorporated into the bigger one. Transmitted plane polarized light; e) barred chondrule with an accretionary rim. Transmitted light, crossed polars; f) barred chondrule with a thick accretionary rim which also covers a grain of Fe-Ni alloy impacted into the chondrule. Transmitted light, crossed polars.

analyses of the plagioclase intergrowing the olivine reveal higher admixtures of MgO (up to more than 1 wt%).

- Fe-Ni alloys are represented by kamacite (5.7–6.4 wt% Ni) and taenite (24.6–25.8 wt% Ni); one analysis shows intermediate Ni contents of 13.58 wt%. The metal grains most often have even oval surfaces at pore boundaries. No significant chemical variation has been found from cores to rims in the grains. Scarce chromite grains display significant chemical admixtures (Table 1).

- Troilite grains, like the metal ones, have regular concave surfaces at pore boundaries. The analyses indicate slightly higher contents, from cores to rims, of chemical admixtures, such as Al and Mn at the expense of Fe.

Summing up, the new microscope observations and microprobe data indicate that:

1. Partial melting (or rather immiscible silicate, metal, and sulfide melts) seems to have played an important role in the formation of the meteorite. The silicate melt was rich

in the albite-oligoclase component. The apparently rapid crystallization of this melt left patchy and lamellar textures in which albite-oligoclase interpenetrates the olivine and pyroxene.

2. Structural features observed on pore surfaces, such as highly irregular grain boundaries of olivine and pyroxene (“cauliflower structures”), and oval grain surfaces of metal and troilite particles may result from an interaction between the solids and pore fluids. This process may have caused resorption and/or partial recrystallization of some phases (small sub- to euhedral crystals on pore surfaces) as well as some chemical modification of the grain margins exposed to volatiles within the pores.

### ORIGIN OF THE PARENT ROCK

The rock of the described texture and composition may have formed on or near the surface of a small asteroid or planetesimal as a result of gravitationally induced and slow accretion of poorly sorted components, which formed the grain framework and minor matrix. The sedimentary medium was of low density and low kinetic energy, as inferred from the poor grain-size sorting. Consequently, the parent rock of the Baszkówka meteorite may be termed a cosmic or asteroid sandstone or planetesimal sandstone.

The most likely environment of the origin of the Baszkówka chondrite parent rock is the zone of gravitational attraction of a small body (an asteroid or planetesimal) directly after a collision with a similar object. The two colliding bodies must have been partly molten with a thin solid crust; alternatively, the collision may have melted considerable parts of the bodies. Incomplete remelting is indicated by the presence of rare and small achondritic fragments and individual olivine crystals in the matrix (Figs. 3c, 3d, and 5). Although these fragments and crystals show no evidence of shock metamorphism, their very presence suggests that part of the material was not remelted. This may have happened if the shock pressure wave during the collision had come well ahead of the thermal front, which is highly probable. In that case, part of the material thrown into the space in the early phase of the collision could have escaped remelting. The aggregates comprising chondrules and/or chondrule fragments must have been aggregated after the collision as they fell back on to the planetesimal; they may also represent unmelted particles thrown into the space during the collision. And, finally, aggregates composed of olivine and pyroxene crystals alone, which are not chondrules or their fragments, must have crystallized in magmatic conditions. Consequently, they represent melted parts of the planetesimals or are derived from the melt which formed during the collision. The post-collisional cloud, comprising mostly molten material, apparently, was dense enough to

prevent rapid cooling and, consequently, to enable the crystallization of chondrules.

The cloud composed of dust and gas that resulted from the collision would have led to poor sorting because of the weak gravitation of a small asteroid. Such an environment should also have a relatively low density (e.g., compared to subaqueous conditions) and low kinetic energy. Thus, a slow falling of particles onto the surface may be seen, and at a high temperature, their welding would produce a strongly porous rock. Thus, the Baszkówka chondrite may be considered a fragment of rock that formed close to the end of such processes and near the surface of the body, so that it escaped strong compaction. Such an environment may have been overlain later by loose regolith.

This scenario for the Baszkówka parent rock is consistent with the chemical variation of metal and troilite grains exposed on pore surfaces, which are interpreted to have resulted from chemical interaction between the solid phases and pore fluid (Borucki and Stępniewski 2001), which most likely occurred during the formation of the rock at the planetesimal surface. Furthermore, the observed depletion of the Baszkówka chondrite in volatile elements (increasing with element mobility), e.g., in Hg, compared to other L chondrites (Dybczyński et al. 1999, 2001a, b) is consistent with this model. Furthermore, the observed growth of secondary (?) olivine and pyroxene crystals into the pore space (Fig. 2d) suggests their crystallization from or interaction with vapor that filled the primary (syndimentary) pores. The absence of serpentinization suggests that the original fluids contained negligible water (and oxygen?) amounts, while they may have contained compounds such as Al, Ca, Na, Fe, Mn, Mg, and others, which resulted in chemical modification of the mineral grain margins exposed to the pores.

Other chondrites displaying porosity similar to that of Baszkówka (e.g., Mount Tazerzait L5 and Nuevo Mercurio H5) are also characterized by well-crystallized textures. This suggests that the particles being accreted were at high temperature and were immediately welded, which enabled the preservation of their porosity.

Our scenario does not fit well with the standard model of chondrule and chondrite formation according to which chondrules form due to flash heating of dust clouds in the solar nebula, and subsequently, as a result of accretion processes, they produce planetesimals. Afterward, thermal metamorphism takes place in these bodies, which causes recrystallization and homogenization of the chemical composition. The resultant rock is equivalent to a metamorphic rock. The metamorphic grade changes with depth and this implies an “onion” model of asteroid (or planetesimal) internal structure (Bennett and McSween 1996). In such a model, only primary chondrules are formed in a protoplanetary disk, and rocks corresponding to the L5

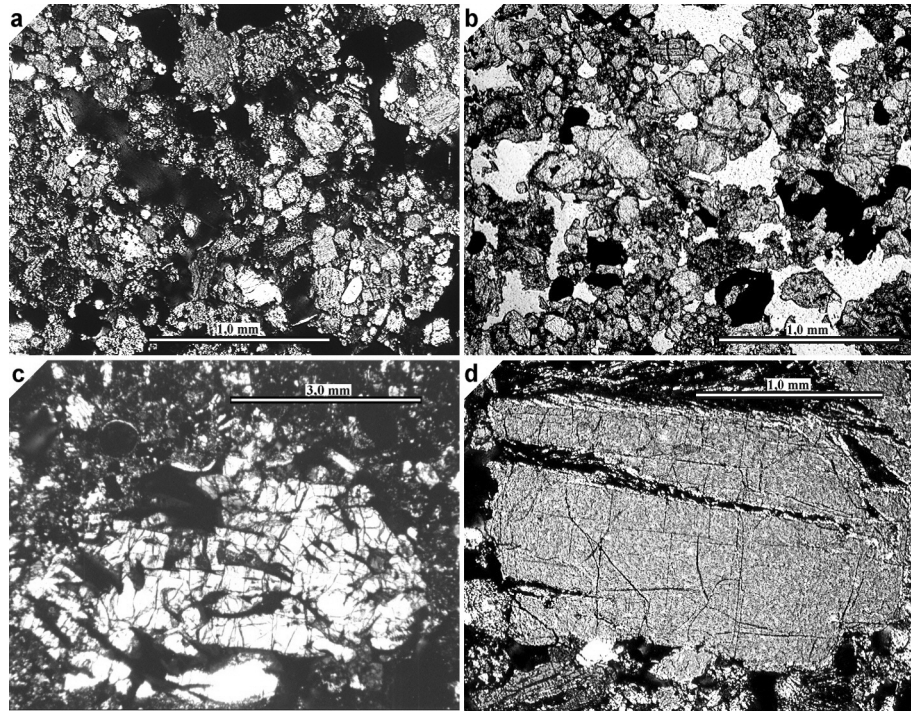


Fig. 5. Achondritic fragments of the meteorite formed before or directly after collision of the partially melted planetesimals: a) and b) small chondrule fragments, olivine crystals, and Fe-Ni alloy forming the meteorite matrix. Transmitted light, crossed polars (a); c) and d) big olivine crystals (phenocrystals). Transmitted light, crossed polars.

type would be found at depths ranging between ten and several tens of km, below which compaction would reduce porosity. However, another model of asteroid internal structure, the “rubble pile” model, invokes an accretionary origin of such bodies due to multiple collision of various fragments of formerly recrystallized planetesimals (asteroids), the structure of which corresponds to the “onion” model described above (Keil et al. 1994). The “rubble pile” model better explains the origin of brecciated meteorites with high shock indices. However, the Baszkówka chondrite does not show shock changes (shock index S1) and, consequently, is not consistent with that model.

A more suitable model for the creation of the Baszkówka meteorite seems to be that proposed by Sanders (1996), partly based on Zook’s (1980) ideas. In this model, the chondrules form during the collision of molten planetesimals, producing a cloud of droplets and dust that become gradually integrated, creating a new planetesimal.

In this case, the compositional homogenization is already attained in the cloud and, in particular, in the near-surface zone of a planetesimal, the likely setting for Baszkówka (Fig. 6). Further recrystallization does not take place. Such a collision between completely or partly melted planetesimals 30–100 km in diameter may often have happened ~1 to 2 Myr after the solar system was formed. A source of energy sufficient to melt planetesimals and to keep them in a liquid

phase is the radioactive decay of  $^{26}\text{Al}$  (Sanders 1996). According to this model, the chondrules in the Baszkówka meteorite would not represent the primary matter of the protoplanetary disk but, rather, secondary material being mixed (perhaps several times) during planetesimal collisions in the earliest stages of evolution of the solar system. A similar scenario for the accretion of secondary chondrules after the collision of partly melted planetesimals in the early solar system, with a significant contribution from the material left from the protoplanetary disk, has been proposed by Hutchison (1996).

Consolomagno (2000) proposed 2 possible scenarios for the lithification processes of the chondrite parent rocks: a) rapid lithification following a collision of planetesimals at moderate speeds, which would not produce significant shock changes; or b) lithification far from the collision site. Both cases were possible only in early stages of the evolution of the solar system when it was not influenced by the gravitational field of large planets such as the Jupiter (Consolomagno 2000). The second scenario envisages a slow lithification of planetesimals, either those with large volume and high porosity due to long-lasting compaction, or smaller-sized bodies with significant chemical reactions between minerals, water, and  $\text{CO}_2$  (Consolomagno 2000). Our model of the origin of the Baszkówka chondrite is yet another possible scenario among collision theories for the lithification of chondrite parent rocks.

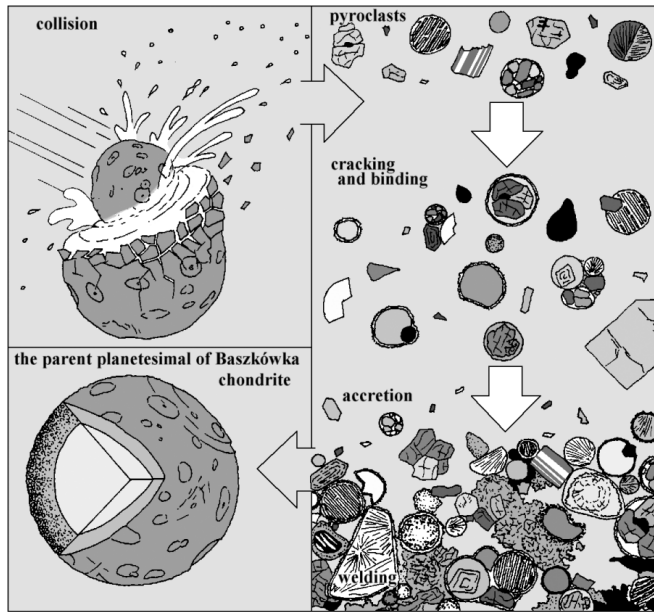


Fig. 6. Cartoon of processes involved in the formation of the Baszkówka L5 chondrite parent rock based on Sanders' (1996) model of the collision of melted planetesimals in the early solar system.

#### SEDIMENTARY ENVIRONMENT OF THE FORMATION OF THE PARENT BODY

In this paper, we have used the terminology devised for terrestrial sedimentary rocks. This is because of strong similarities between the Baszkówka meteorite and sedimentary rocks, which are obvious from microscopic observations of the chondrite. The collision and its direct effects may be compared to erosion. The collision threw largely melted material into space, a process equivalent to sedimentary transport in the terrestrial environment. The settling of this material is comparable with the deposition of pyroclastic rocks. Similar ideas have been proposed by Tschermak (1875), Merrill (1930), and Wahl (1952), but these authors suggested further-reaching analogies with terrestrial processes, considering chondrules as volcanic eruption products on the parent planets of chondrites (Maneck 1972). According to other concepts (Ramdohr 1967), the formation of chondrules (those made of chromite, for instance) and their subsequent aggregation may be explained by early rapid cooling followed by a slower cooling, as in tuffs deposited in terrestrial conditions.

Similarly, the welding of particles and possible binding of rock fragments by liquid or plastic Fe-Ni alloys and sulfides can be compared with the welding and subsequent diagenesis of terrestrial pyroclastic rocks (Fig. 7).

#### SUMMARY AND CONCLUSION

Textural features of the Baszkówka L5 chondrite suggest that its parent body formed in an environment similar to that in which terrestrial pyroclastic rocks are deposited. This

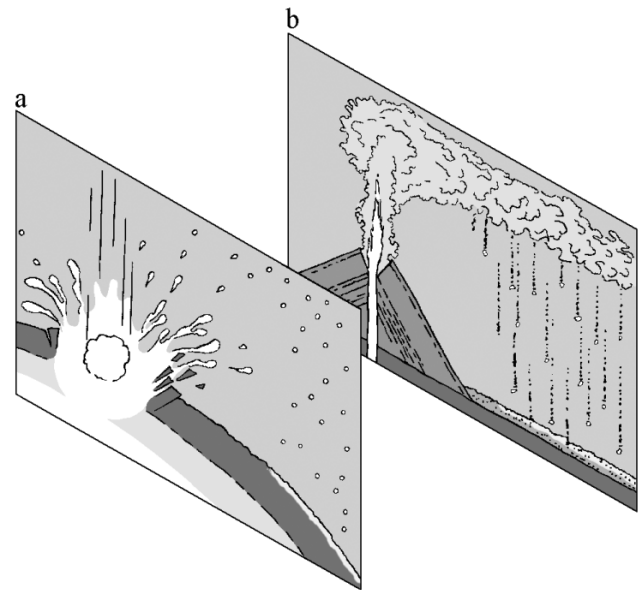


Fig. 7. Comparison of the formative processes of the Baszkówka meteorite to equivalent terrestrial pyroclastic-rock forming processes. The former process, shown in (a), is of global character, while the latter one, shown in (b), is of regional extent. The scales of the two drawings are different.

particularly applies to the accretion and lithification processes involved. However, the origin of chondrules and achondritic fragments (olivine and pyroxene crystal aggregates), as well as chondritic-achondritic aggregates, are consistent with a model of a collision of 2 melted or partially melted planetesimals possessing a thin crust. Such a process probably happened at an early stage in the evolution of the solar system, between 1 and 2 Myr after its creation. A collision of at least partially liquid planetesimals produced a cloud from which secondary chondrules crystallized, but which also contained products of earlier magmatic crystallization (achondrite fragments). In the collision cloud, broken chondrules, compound chondrules, and aggregates composed of chondrules and their fragments were formed. In that low-density and low-energy environment, all these components were accreted onto the surface of the larger of the 2 collided planetesimals due to its greater gravitational attraction. The density of the medium was low enough to lead to inefficient grain-size sorting, but was high enough to prevent fast cooling and, as a result, to enable interparticle welding. The meteorite parent rock was, apparently, already homogenized while in the cloud and, particularly, in the near-surface zone of the planetesimal. The hot material settling on the planetesimal surface became welded and, additionally, still-liquid or at least plastic grains of metal and sulfides bonded the grains of the framework and the minor matrix. The process resembled the lithification of pyroclastic rocks. After the rock was formed on the surface of the planetesimal, no further recrystallization of the chondrite occurred. The significant porosity of the Baszkówka meteorite indicates that

it represents a fragment from the shallow, subsurface zone of a planetesimal. Rocks of similar composition but derived from a greater depth would have been more strongly compacted, as in the case of the Mt. Tazerzait L5 chondrite (Pilski et al. 2001).

The proposed model is not thought to be a general formation mechanism of ordinary chondrites. Both meteorites, Baszkówka and Mt. Tazerzait, are termed “unusual” (Wlotzka et al. 1997), so they need an unusual explanation of origin. We think, however, that the explanation presented here could be a specific case of a general process suggested by Hutchison (1996) and Sanders (1996).

*Acknowledgments*—Ryszard Kryza acknowledges financial support from an internal grant of Wrocław University, 2022/W/ING/01–17. The Microscan M9 in the Department of Mineralogy and Petrology, Wrocław University, was donated by the Free University of Amsterdam. Henryk Siagło is thanked for his help with microprobe work, and Jan Zalasiewicz for his valuable comments and improvements of an earlier version of the manuscript.

*Editorial Handling*—Dr. Carlé Pieters

## REFERENCES

- Bennett M. E. and McSween H. Y., Jr. 1996. Revised model calculations for the thermal histories of ordinary chondrite parent bodies. *Meteoritics & Planetary Science* 31:783–792.
- Borucki J. and Stępniewski M. 2001. Mineralogy of the Baszkówka chondrite (L5 S1): New data on silicates, opaques, and minor minerals. *Geological Quarterly* 45:229–255.
- Consolomagno G. J. 2000. Lithification scenarios for ordinary chondrites. *Meteoritics & Planetary Science* 35:A45.
- Dybczyński R., Danko B., Kulisa K., Polkowska-Motrenko H., Samczyński Z., Stępniewski M., and Szopa Z. 1999. First chemical characterisation of the new Polish meteorite “Baszkówka” by neutron activation analysis. *Chemia Analityczna* 44:471–484.
- Dybczyński R., Borucki J., Danko B., Kulisa K., Polkowska-Motrenko H., Samczyński Z., Stępniewski M., Szopa Z., and Tanida K. 2001a. The investigation of genetic relationship between the Baszkówka and Mt. Tazerzait chondrites by NAA and other methods. *Chemia Analityczna* 46:477–488.
- Dybczyński R., Chwastowska J., Danko B., Kulisa K., Polkowska-Motrenko H., Samczyński Z., Sterlińska E., and Szopa Z. 2001b. A study on chemical composition of Baszkówka and Mt. Tazerzait chondrites. *Geological Quarterly* 45:289–301.
- Hutchison R. 1996. Chondrules and their associates in ordinary chondrites: A planetary connection? In *Chondrules and the protoplanetary disk*, edited by Hewins R. H., Jones R. H., and Scott E. R. D. Cambridge: Cambridge University Press. pp. 311–318.
- Keil K., Haack H., and Scott E. R. D. 1994. Catastrophic fragmentation of asteroids: Evidence from meteorites. *Planetary and Space Science* 42:1109–1122.
- Manecki A. 1972. Chondrules and chondrites. *Prace Mineralogiczne* 27:7–52. In Polish.
- Merill G. P. 1930. Composition and structure of meteorites. *Bulletin of the United States National Museum* 149.
- Pilski A. S., Przylibski T. A., and Zagożdżon P. P. 2001. Comparative analysis of the Baszkówka and Mt. Tazerzait chondrites: Genetic conclusions based on astrophysical data and the mineralogical and petrological data. *Geological Quarterly* 45:331–342.
- Przylibski T. A. and Zagożdżon P. P. 1999. Baszkówka—a cosmic sandstone. *Mineralogical Society of Poland—Special Papers* 14: 113–115.
- Ramdohr P. 1967. Chromite and chromite chondrules in meteorites. *Geochimica et Cosmochimica Acta* 31:1961–1967.
- Sanders I. S. 1996. A chondrule forming scenario involving molten planetesimals. In *Chondrules and the protoplanetary disk*, edited by Hewins R. H., Jones R. H., and Scott E. R. D. Cambridge: Cambridge University Press. pp. 327–334.
- Siemiątkowski J. 2001. Petrography of the Baszkówka chondrite. *Geological Quarterly* 45: 263–280.
- Stępniewski M., Borucki J., and Siemiątkowski J. 1998. New data on the L5 (S1) chondrite Baszkówka (Poland). *Meteoritics & Planetary Science* 33:A150–A151.
- Stępniewski M., Radlicz K., Siemiątkowski J., and Borucki J. 1996. Preliminary study of the L chondrite Baszkówka (Poland). *Meteoritics & Planetary Science* 31:A134–A135.
- Stępniewski M., Siemiątkowski J., Borucki J., and Radlicz K. 1997. Fall, recovery, and preliminary study of the Baszkówka meteorite (Poland). *Archiwum Mineralogiczne* 51(1–2):131–152.
- Tschermak G. 1875. *Die Bildung der Meteoriten und der Vulkanismus*. Wien: Akademie der Wissenschaften. 71 p.
- Wahl W. 1952. The brecciated stony meteorites containing foreign fragments. *Geochimica et Cosmochimica Acta* 2:91–117.
- Wlotzka F., Scherer P., Schultz L., Otto J., and Stępniewski M. 1997. Petrography and noble gases of the unusual L5 chondrites Baszkówka and Mt. Tazerzait. *Meteoritics & Planetary Science* 32:A140–A141.
- Wlotzka F. and Otto J. 2001. Euhedral crystals in interstitial pores of the Baszkówka and Mt. Tazerzait L5 chondrites. *Geological Quarterly* 45:257–262.
- Zook H. A. 1980. A new impact model for the generation of ordinary chondrites. *Meteoritics* 15:390–391.